



Comparison between the Improved Sequence Network Model of wind turbines and the Classical Model based on Sequence Networks for short-circuit studies



Jamer A. González-Vásquez, Nicolás Toro, Jorge F. Gutierrez

Universidad Nacional de Colombia
Sede Manizales

jaagonzalezva@unal.edu.co, ntoroga@unal.edu.co, jfernando@ieee.org

Abstract

Space vector theory is a widely used tool to model synchronous and asynchronous machines. In this poster the induction machine dynamic equations were written in terms of space vectors, employing the stationary reference frame. Also, a general short-circuit current expression was derived and decomposed into positive and negative sequence components. In order to validate and compare the model developed with a simplified model found in literature, short-circuit simulations with balanced and unbalanced sources were performed. The results shown that, for some cases, the mismatches between those approaches are relevant and cause some problems during design, coordination of protection and control stages of machine systems. Discrete Fourier Transform (DFT) and mean squared error (MSE) were used to accomplish this comparison. Finally, a different approach for modeling sequence voltages was proposed and compared with the two methodologies aforementioned.

1. Equations for short-circuit current

The state equation is written in space vector notation as:

$$\frac{d}{dt} \begin{bmatrix} \vec{\lambda}_s \\ \vec{\lambda}_r \end{bmatrix} = \begin{bmatrix} -\frac{R_s}{L'_s} & \frac{R_s L_m}{L'_s L_r} \\ \frac{R_r L_m}{L'_r L_s} & -\frac{R_r}{L'_r} + j\omega_r \end{bmatrix} \begin{bmatrix} \vec{\lambda}_s \\ \vec{\lambda}_r \end{bmatrix} + \begin{bmatrix} \vec{v}_s \\ \vec{v}_r \end{bmatrix} \quad (1)$$

The solution of (1) is then:

$$\vec{\lambda}_s = \frac{p_1 (\vec{\lambda}_{si} - p_2 \vec{\lambda}_{ri}) e^{\psi_1(t-t_0)}}{p_1 - p_2} + \frac{p_2 (p_1 \vec{\lambda}_{ri} - \vec{\lambda}_{si}) e^{\psi_2(t-t_0)}}{p_1 - p_2} + \vec{\Lambda}_{1s} e^{j\omega_s t} + \vec{\Lambda}_{2s} e^{-j\omega_s t} \quad (2)$$

$$\vec{\lambda}_r = \frac{(\vec{\lambda}_{si} - p_2 \vec{\lambda}_{ri}) e^{\psi_1(t-t_0)}}{p_1 - p_2} + \frac{(p_1 \vec{\lambda}_{ri} - \vec{\lambda}_{si}) e^{\psi_2(t-t_0)}}{p_1 - p_2} + \vec{\Lambda}_{1r} e^{j\omega_s t} + \vec{\Lambda}_{2r} e^{-j\omega_s t} \quad (3)$$

A short-circuit current equation can be determined using (3):

$$\vec{i}_s = \vec{I}_{dc} e^{\psi_1(t-t_0)} + \vec{I}_t e^{\psi_2(t-t_0)} + \vec{I}_{ss} e^{j\omega_s t} \quad (4)$$

where:

$$\vec{I}_{dc} = \frac{(\vec{\lambda}_{si} - p_2 \vec{\lambda}_{ri}) (p_1 - \frac{L_m}{L_r})}{L'_s (p_1 - p_2)} \quad (5)$$

$$\vec{I}_t = \frac{(p_1 \vec{\lambda}_{ri} - \vec{\lambda}_{si}) (p_2 - \frac{L_m}{L_r})}{L'_s (p_1 - p_2)} \quad (6)$$

$$\vec{I}_{ss} e^{j\omega_s t} = \left[\left(\frac{\vec{\Lambda}_{1s}}{L'_s} - \frac{L_m}{L_r L'_s} \vec{\Lambda}_{1r} \right) - \left(\frac{\vec{\Lambda}_{2s}}{L'_s} - \frac{L_m}{L_r L'_s} \vec{\Lambda}_{2r} \right) \right]^* e^{j\omega_s t} \quad (7)$$

Another approach for the steady state component is given by:

$$\vec{i}_s = \vec{I}_{dc} e^{\psi_1(t-t_0)} + \vec{I}_t e^{\psi_2(t-t_0)} + \vec{I}_{ss1} e^{j\omega_s t} + \vec{I}_{ss2} e^{-j\omega_s t} \quad (8)$$

$$\vec{I}_{ss1} e^{j\omega_s t} = \left(\frac{\vec{\Lambda}_{1s}}{L'_s} - \frac{L_m}{L_r L'_s} \vec{\Lambda}_{1r} \right) e^{j\omega_s t} \quad (9)$$

$$\vec{I}_{ss2} e^{-j\omega_s t} = \left(\frac{\vec{\Lambda}_{2s}}{L'_s} - \frac{L_m}{L_r L'_s} \vec{\Lambda}_{2r} \right) e^{-j\omega_s t} \quad (10)$$

2. Results

In this section short-circuit current calculation of (8) and (4) are compared against each other using simulations of symmetrical and asymmetrical faults.

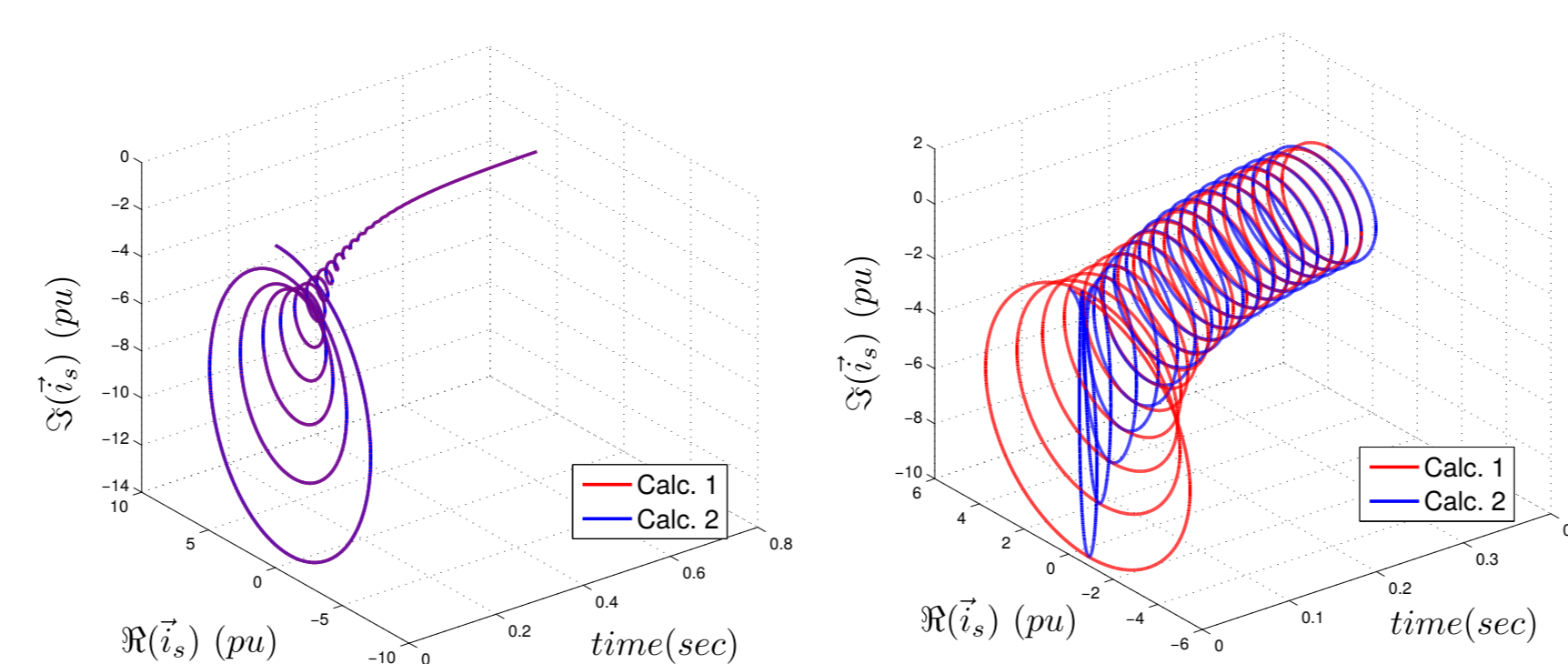


Figure 1: Symmetrical and asymmetrical faults - 3D view.

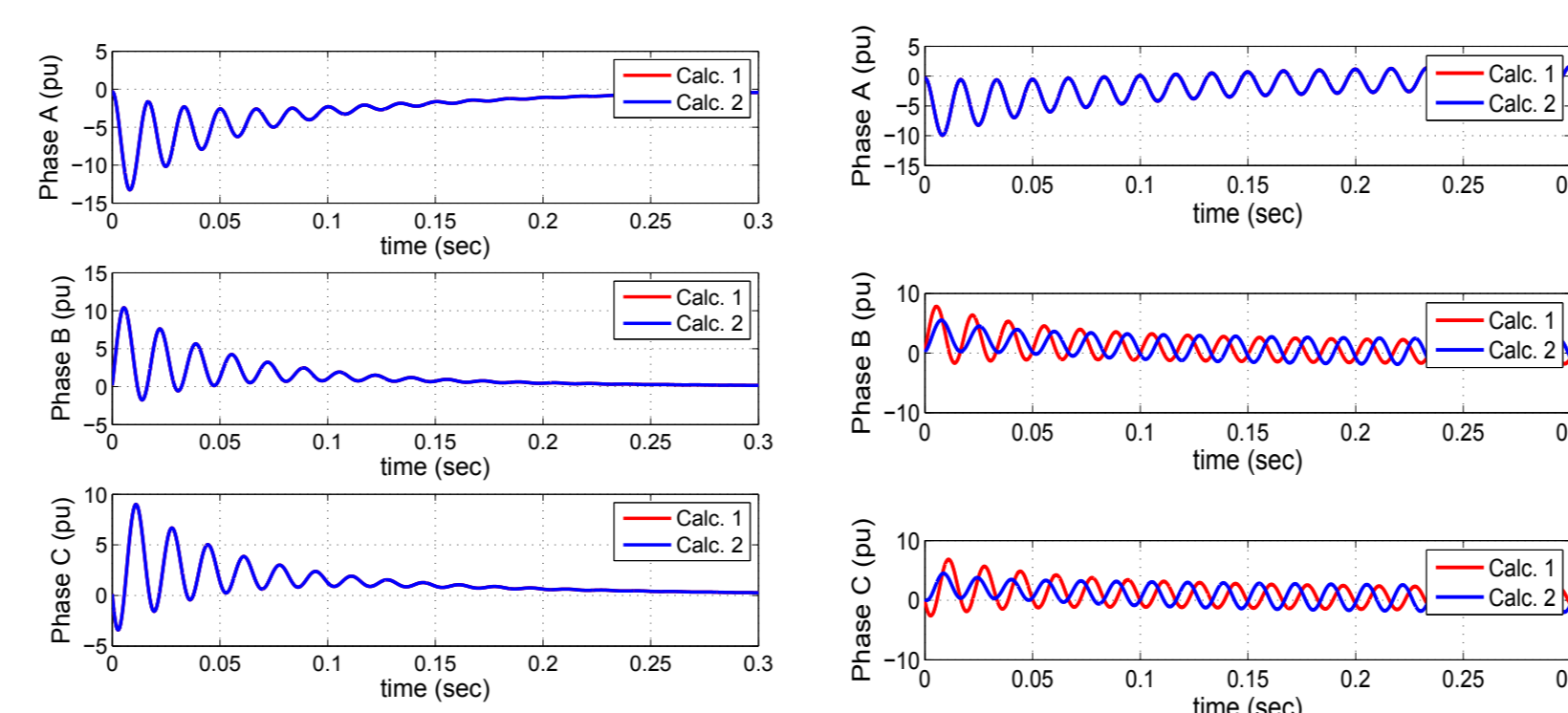


Figure 2: Instantaneous short-circuit current for symmetrical and asymmetrical faults.

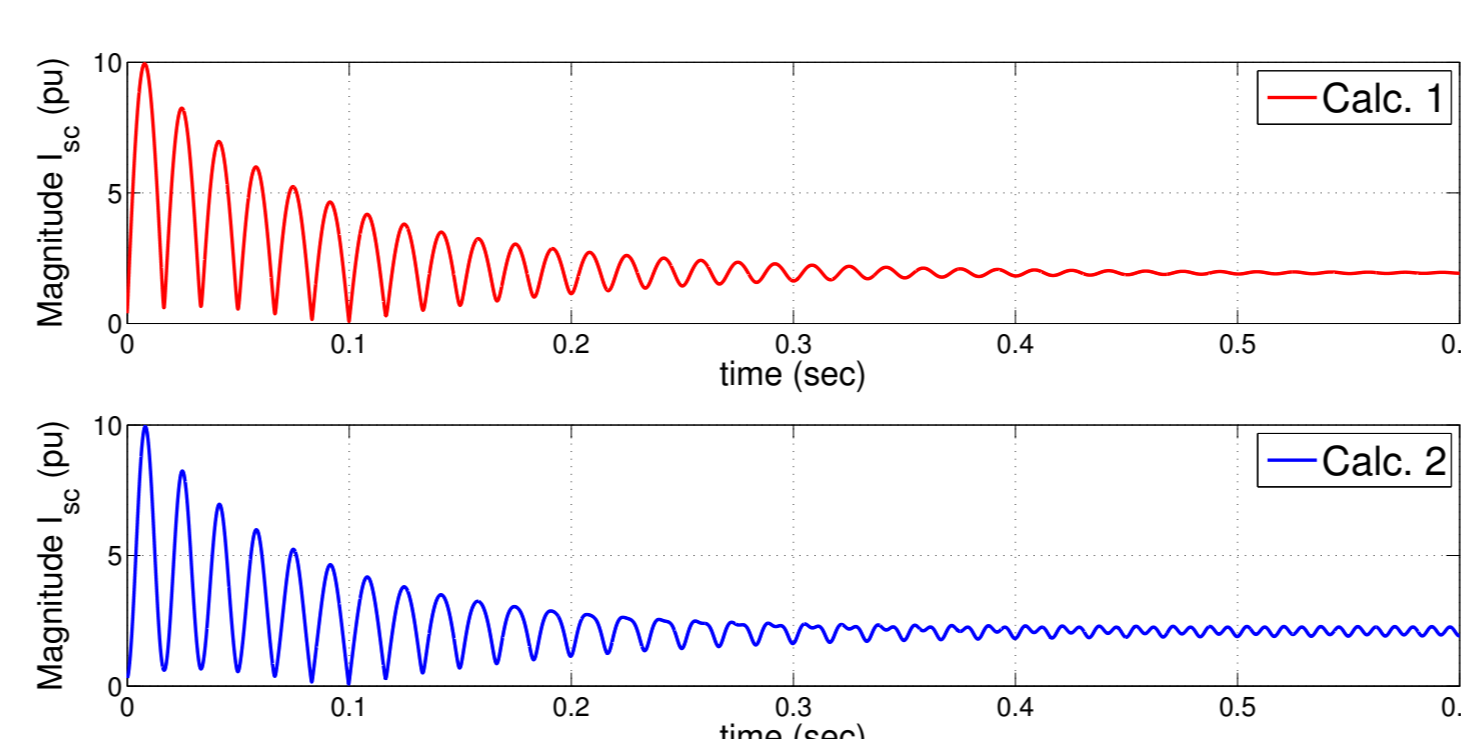


Fig. 3: Magnitude of short-circuit current - Phase A to ground fault.

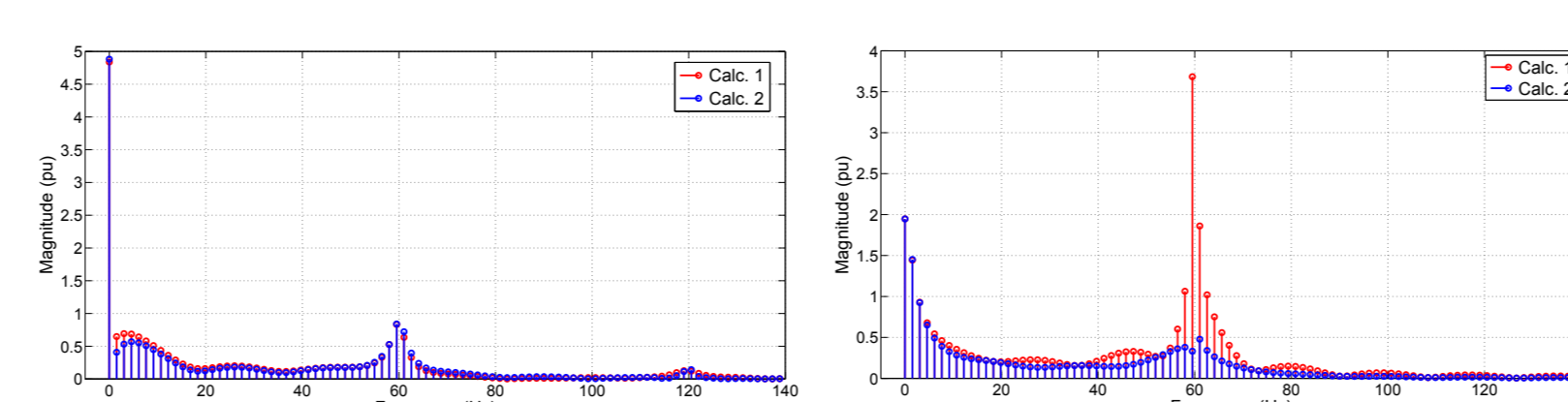


Figure 4: Fourier representations of the space vector short-circuit current and its magnitude.

3. Induction Machine Sequence Network Representation

3.1 Classical equations

The following equations are used to calculate both symmetrical and asymmetrical faults.

$$X' = j\omega_s L'_s \quad (11)$$

$$V' = j\omega_s \frac{L_m}{L_r} \vec{\lambda}_r \quad (12)$$

3.2 Improved Sequence Model (ISM)

The equation for symmetrical faults is given by:

$$V' = \frac{j\omega_s L_m}{L_r (p_1 - p_2)} [p_1 \Lambda_r^b - \Lambda_s^b] \quad (13)$$

Equations for asymmetrical faults are:

$$V'_1(\delta) = \frac{j\omega_s L_m p_1 (\Lambda_r^b - \Lambda_r^{a+} + \Lambda_r^{a-*} e^{-j2\delta})}{L_r (p_1 - p_2)} - \frac{j\omega_s L_m (\Lambda_s^b - \Lambda_s^{a+} + \Lambda_s^{a-*} e^{-j2\delta})}{L_r (p_1 - p_2)} + j\omega_s \frac{L_m}{L_r} \Lambda_r^{a+} \quad (14)$$

$$V'_2 = j\omega_s \frac{L_m}{L_r} \Lambda_r^{a-} \quad (15)$$

3.3 Proposed Sequence Model (PSM)

The equation for symmetrical faults is given by:

$$V' = j\omega_s \frac{L_m}{L_r} \Lambda_r^b \quad (16)$$

Equations for asymmetrical faults are:

$$V'_1 = j\omega_s \frac{L_m}{L_r} [\Lambda_r^b + \Lambda_r^{a-*}] \quad (17)$$

$$V'_2 = -j\omega_s \frac{L_m}{L_r} \Lambda_r^{a-} \quad (18)$$

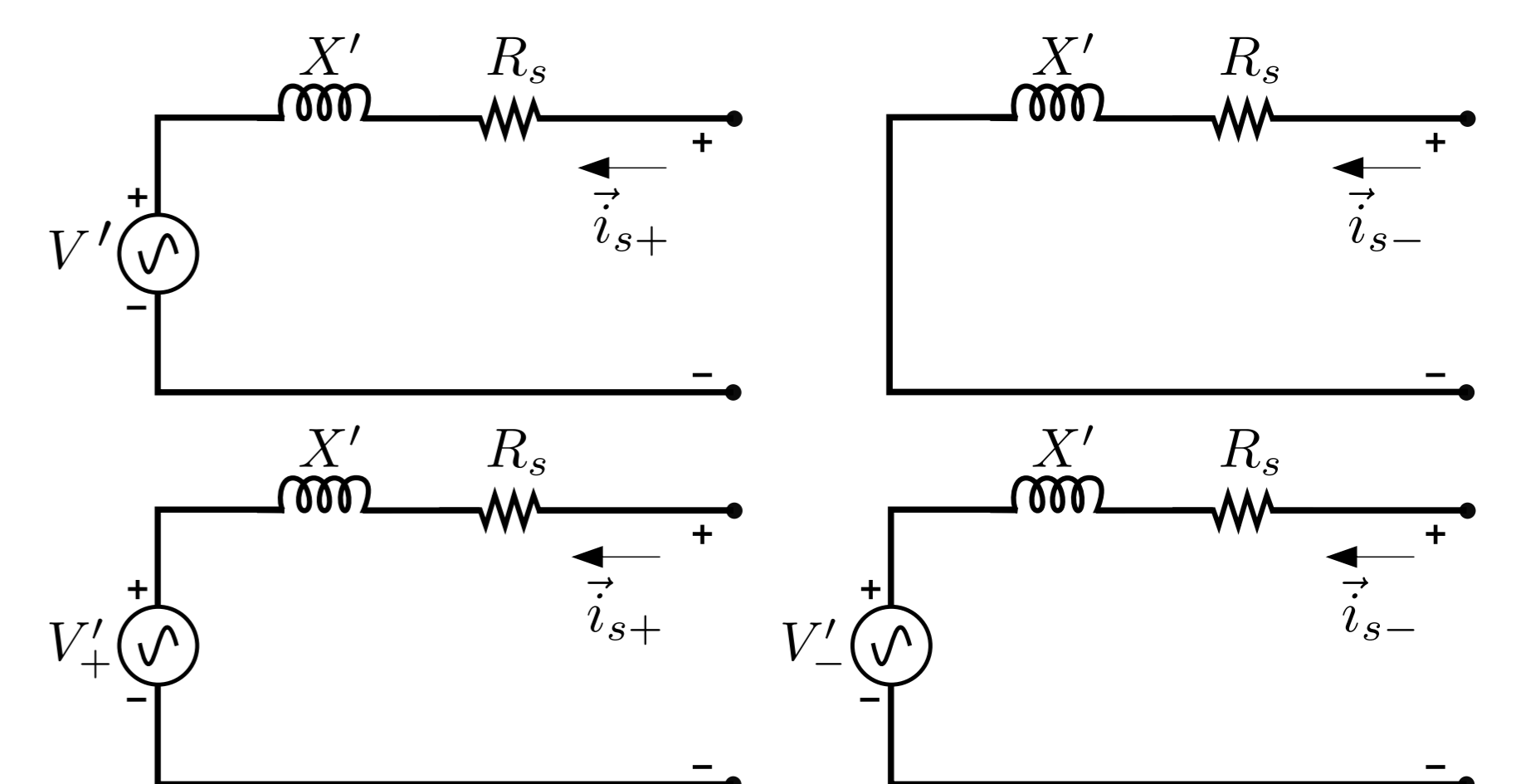


Figure 5: Sequence networks components of induction machine, using the improved and classical model.

4. Conclusions

There is a discrepancy between (4) and (8) induction machine short-circuit currents, except for the symmetrical fault, where the steady state component does not exist. The differences are due to the fact that the negative sequence component in (6) was factorized improperly. The greatest MSE for short-circuit current magnitudes between those approaches were found close to synchronous frequency for all kind of faults considered. However, the main discrepancy lies in the phase shifts of short-circuit currents. The 120 Hz component is a consequence of the elliptical form of the short-circuit current space vectors in asymmetrical fault cases. It was found that if the machine is connected to an asymmetrical source the differences between the approaches increase significantly, e.g. the case of phase A to ground fault the MSE was 39.2%. In consequence, the steady state part of short-circuit current space vector lies variations in magnitudes and phase shifts of the instantaneous phase currents. The 3D view of the short-circuit space vectors displayed in Fig. 1, allows to understand induction machine short-circuit currents behavior and its representation both in space and time frames. The symmetrical component analysis of induction machines presents enough accuracy for balanced faults but for asymmetrical ones could result in inaccuracies. Those improved models analyzed in this work (ISM and PSM) have a better performance, however the PSM implies a process with easier calculations and more accurate short-circuit current magnitude values. The proposed short-circuit current (8), and the voltage behind transient reactance expressions (16), (17) and (18) could avoid some problems in design, coordination of protection devices and in machine control analysis.